ISBN: 978-3-95450-248-6 ISSN: 2673-5490 doi: 10.18429/JACoW-IPAC25-TUPM089

TWIN-BUNCH MODELLING IN LINEAR ACCELERATORS FOR PLASMA WAKEFIELD ACCELERATION

T. Long*, L. Boulton, Y. Chen, W. Decking, M. Scholz, S. Wesch, J. C. Wood,
Deutsches Elektronen-Synchrotron, DESY, Hamburg, Germany
J. Björklund Svensson, Lund University, Lund, Sweden

Abstract

Twin electron bunches accelerated by high-energy linacs are attracting increasing interest especially in twin free-electron laser (FEL) pulse generation and beam-driven plasma wakefield acceleration (PWFA) studies. High-energy linacs may benefit from plasma accelerators, where a trailing bunch is accelerated in GV/m fields in a plasma wave driven by the leading bunch. This could facilitate high-energy physics, as well as greatly increase the available photon energy range of existing FELs without increasing the footprint. Here, initial analytical studies of twin-bunch generation in FLASH accelerator are carried out. With the initial beam longitudinal phase space properly tuned by temporally shaping the photocathode laser, together with optimizing linac settings, high-quality twin electron bunches with tunable delay and simultaneous bunch shaping can be generated, which is essential for energy-efficient PWFA with low energy spread.

INTRODUCTION

Twin electron bunch generation in high-energy linacs is attracting increasing interest especially in twin free-electron laser (FEL) pulse generation and beam-driven plasma wakefield acceleration (PWFA) studies [1–5]. Combining the advantage of the superconducting accelerator technology with the cutting-edge compact PWFA can boost electron beam energy with high beam quality without increasing the linac footprint [6, 7], which may extend the beam energy range or maintain the beam energy after a high-duty cycle upgrade of linac, where beam energy may drop a lot due to cooling constraints to linac [8].

Twin electron bunches with a separation of 100 μm level are needed for beam-driven PWFA. For machines operating in low average power mode, bunch pairs of adjustable bunch length and separation can be generated by energy collimators in a dispersive section [9]. However, the dumped energy gets high and may damage the collimator in high-repetition rate operation mode with a large number of electron bunches, and a direct generation of twin bunches from the photocathode is necessary to enable beam-driven PWFA with high average power. In addition, strong beam loading of plasma wakefields with carefully tailored bunch current profiles is necessary for energy-efficient PWFA with low energy spread [10–13].

In this paper, a modelling study of twin-bunch acceleration starting from the photocathode within one rf bucket is carried out for linac with multistage compression. It is shown that by utilizing a temporally shaped photoinjector laser, current profiles can be tailored into trapezoidal shapes by tuning the linac compression properly. Start-to-end simulation studies for FLASH [14, 15] accelerator show that the optimized accelerated bunches are shaped in current profiles with a typical delay between the two bunches suitable for PWFA.

TWIN BUNCH MODELLING

Longitudinal beam dynamics for the acceleration of twin bunches is described following the formalism presented in [16–18]. The relative particle longitudinal coordinate within the bunch is noted as s at the gun exit, and the reference particle has a coordinate of s_0. The particle has a longitudinal coordinate S_{BC} after the bunch compressor BC, which can be approximated as

$$S_{\mathrm{BC}}(s) \approx S^0_{\mathrm{BC}} + Z^0_{\mathrm{BC}}(s-s_0) + \frac{Z'^0_{\mathrm{BC}}}{2}(s-s_0)^2 + \frac{Z''^0_{\mathrm{BC}}}{6}(s-s_0)^3 \quad (1)$$

The compression function can be defined as $C_{\mathrm{BC}} = 1/Z_{\mathrm{BC}}$, where $Z_{\mathrm{BC}} = \partial S_{\mathrm{BC}}/\partial s$. Given the initial current profile at the gun exit $I_0(s)$ and the longitudinal coordinate evolution $S_{\mathrm{BC}}(s)$, one can obtain the current profile after BC as $I_{\mathrm{BC}}(S_{\mathrm{BC}})$. In ref [16], Z_{BC} is expanded as a polynomial of s. Here we expand C_{BC} as a polynomial of S_{BC}, and this new treatment has the advantage of precisely describing the final current profile after the bunch compressor. When $s(S_{\mathrm{BC}})$ is a single-valued function, we can expand s over S_{BC} as

$$s(S_{\mathrm{BC}}) \approx s_0 + C^0_{\mathrm{BC}}(S_{\mathrm{BC}} - S^0_{\mathrm{BC}}) + \frac{C'^0_{\mathrm{BC}}}{2}(S_{\mathrm{BC}} - S^0_{\mathrm{BC}})^2 + \frac{C''^0_{\mathrm{BC}}}{6}(S_{\mathrm{BC}} - S^0_{\mathrm{BC}})^3, \quad (2)$$

and we have

$$C_{\mathrm{BC}}(S_{\mathrm{BC}}) \approx C^0_{\mathrm{BC}} + C'^0_{\mathrm{BC}}(S_{\mathrm{BC}} - S^0_{\mathrm{BC}}) + \frac{C''^0_{\mathrm{BC}}}{2}(S_{\mathrm{BC}} - S^0_{\mathrm{BC}})^2. \quad (3)$$

For a flat-top initial current profile with current of I_0, as shown by the solid curve in the first row of Fig. 1, we have $I_{\mathrm{BC}}(S_{\mathrm{BC}}) = I_0 \cdot C_{\mathrm{BC}}(S_{\mathrm{BC}})$. For energy-efficient PWFA with low energy spread, strong beam loading of plasma wakefields is required [10–13], where trapezoidal current profiles are preferred. Trapezoidal current profile can be obtained with non-zero C^0_{BC} and C'^0_{BC}, and with C''^0_{BC} being

* tianyun.long@desy.de

ISBN: 978-3-95450-248-6 ISSN: 2673-5490 doi: 10.18429/JACoW-IPAC25-TUPM089

zero, namely a flat-top current profile being compressed with linear compression factor along the final bunch longitudinal coordinate S_{BC}, as shown in the second row of Fig. 1, where we have $C^0_{\mathrm{BC},1} = C^0_{\mathrm{BC},2} = 50$, $C'^0_{\mathrm{BC},1} = -5\times10^5\ \mathrm{m}^{-1}$, $C'^0_{\mathrm{BC},2} = 5\times10^5\ \mathrm{m}^{-1}$, $C''^0_{\mathrm{BC},1} = C''^0_{\mathrm{BC},2} = 0\ \mathrm{m}^{-2}$, with 1 and 2 denote the leading and trailing bunches, respectively. $S_{\mathrm{BC}}(s)$ and $s(S_{\mathrm{BC}})$ are shown by the dashed curves in Fig. 1.

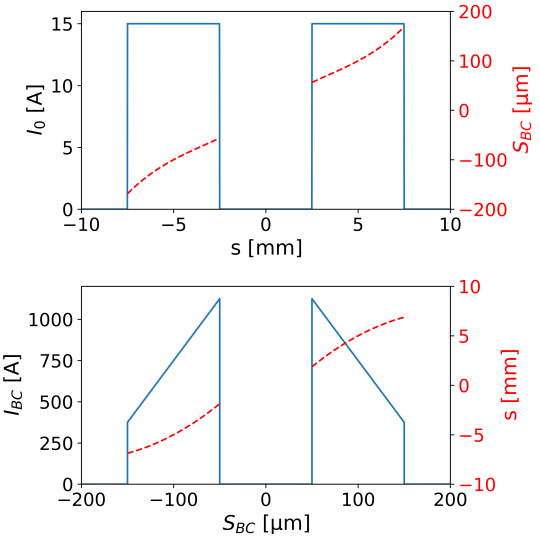

Figure 1: Current profile shaping. First row: initial current profile $I_0(s)$ (solid curve) and $S_{\mathrm{BC}}(s)$ (dashed curve). Delay between the bunch centers is 10 mm. Second row: current profile after compression $I_{\mathrm{BC}}(S_{\mathrm{BC}})$ and $s(S_{\mathrm{BC}})$. Delay between the bunch centers is 200 μm. Head is to the right.

Linac settings should be fine-tuned to get the desired current profiles. Here we consider the longitudinal beam dynamics for FLASH linac, which contains interleaved rf sections and bunch compressors.

The initial electron relative energy offset at the gun exit is expressed as

$$\delta_0(s) = \frac{E_{\mathrm{gun}}(s) - E^0_0}{E^0_0} \approx \zeta_0 + \zeta_1(s-s_0) + \frac{\zeta_2}{2}(s-s_0)^2 + \frac{\zeta_3}{6}(s-s_0)^3 \quad (4)$$

with E^0_0 the reference energy. Electron energy gain from rf cavity is

$$\Delta E_{\mathrm{rf}}(S) = eV_{\mathrm{rf}}\cos(k_{\mathrm{rf}}S + \varphi_{\mathrm{rf}}) \quad (5)$$

with S the particle longitudinal coordinate in the rf, V_{rf} and φ_{rf} are the on-crest rf voltage and phase, k_{rf} is the rf angular wavenumber. For the bunch compressor with momentum compaction factors of R_{56}, T_{566}, U_{5666}, electron longitudinal coordinate evolves as

$$S_{\mathrm{i}} = S_{\mathrm{i-1}} - (R_{56}\delta_{\mathrm{rf}} + T_{566}\delta^2_{\mathrm{rf}} + U_{5666}\delta^3_{\mathrm{rf}}) \quad (6)$$

where $S_{\mathrm{i-1}}$ and S_{i} are the longitudinal coordinate before and after the bunch compressor, δ_{rf} is the electron relative energy offset at the bunch compressor entrance.

We repeat the above treatment for acceleration and compression for the interleaved linac sections. There are 6 rf parameters (rf amplitude and phase: V_{11} and ϕ_{11} for the booster, V_{13} and ϕ_{13} for the third harmonic cavity, V_2 and ϕ_2 for the cavity in between the first bunch compressor BC1 and the second bunch compressor BC2) which can be tuned till BC2 end and we can choose 6 equivalent beam longitudinal phase space parameters representing the acceleration and compression process. For the shaping and delay control, we choose (E^0_{13}, E^0_2, C^0_{BC1}, C^0_{BC2}, C'^0_{BC2}, C''^0_{BC2}) as target compression parameters, rf parameters are obtained from these 6 parameters from the model.

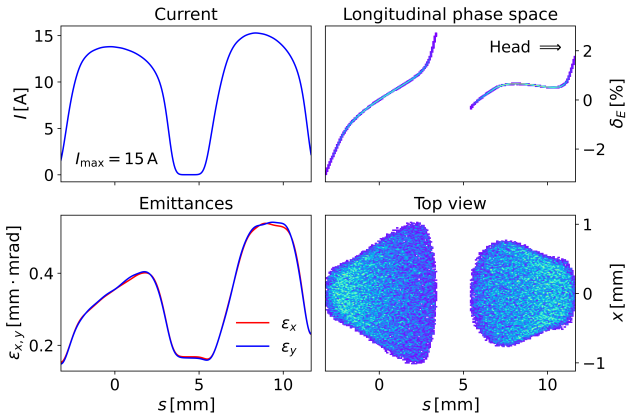

Figure 2: Twin-bunch distribution at the gun exit.

The initial twin-bunch distribution at gun exit with charge of 250 pC for each bunch is simulated with ASTRA [19] and shown in Fig. 2, where two photocathode lasers with uniform longitudinal distribution of 15 ps width, an aperture diameter of 1.15 mm, and a delay between the two pulses of 36 ps are adopted. For convenience, the leading and trailing bunches in Fig. 2 are denoted as bunch 1 and bunch 2, respectively. The fitted parameters for the relative energy offset are tabulated in Table 1.

The compression tuning for bunch 2 is shown in Fig. 3 by changing C^0_{BC1} and C'^0_{BC2}. The rf parameters can be calculated by the model given the target compression of bunch 2, then the compression parameters of bunch 1 can also be calculated by the model with these rf parameters. Here delay is defined as the distance between bunch 1 and bunch 2 after BC2: $S^0_{\mathrm{BC2},1} - S^0_{\mathrm{BC2},2}$, where positive delay means bunch 1 also locates in front of bunch 2 after BC2, negative delay means the relative position of the two bunches is shifted after BC2 compared with their initial relative position shown in Fig. 2. One can see that the current profile shaping and delay between the two bunches can be tuned accordingly, and for the initial twin-bunch distribution considered here, the relative bunch position can be changed for a large (C^0_{BC1}, C'^0_{BC2}) parameter space, where the overcompression can be a reasonable choice for this specific working point [18].

ISBN: 978-3-95450-248-6 ISSN: 2673-5490 doi: 10.18429/JACoW-IPAC25-TUPM089

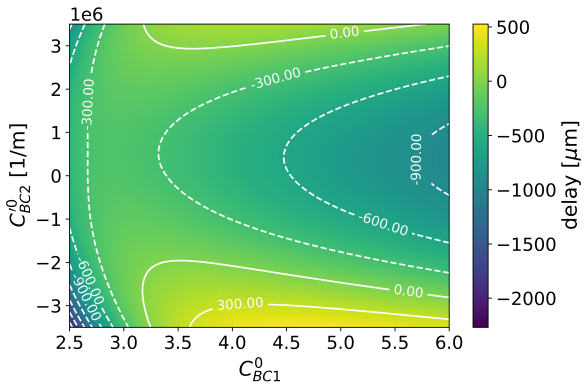

Figure 3: Contour plot of delay between the two bunches over different compression parameters of bunch 1.

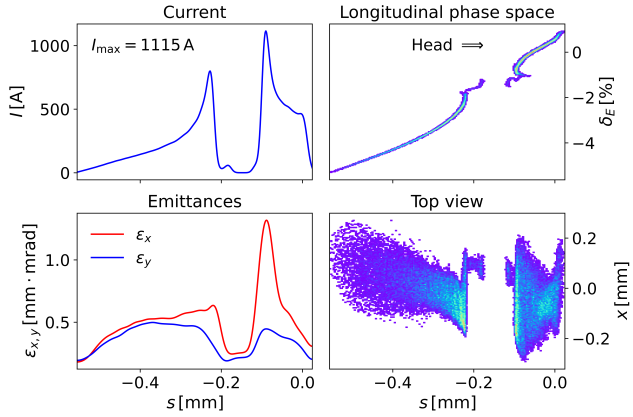

Figure 4: Twin-bunch distribution after the final bunch compressor BC2.

START-TO-END SIMULATION

Start-to-end simulations based on the FLASH linac are carried out with the multi-physics software package OCELOT [20], where collective effects such as coherent synchrotron radiation, space charge, and geometrical wakefields are included in the beam tracking process. An iterative procedure for the simulation [16] is utilized with initial rf parameters obtained based on the twin-bunch model presented in the previous section.

The twin-bunch distribution shown in Fig. 2 is used as the input distribution, and the start-to-end parameters are listed in Table 1. Before the final bunch compressor BC2, bunch 1 (with reference particle position of 2.8 mm and peak current of 30 A) is still located ahead of bunch 2 (with reference particle position of -0.08 mm and peak current of 65 A). The relative position of the two bunches is shifted after BC2 and the twin-bunch distribution is shown in Fig. 4, where bunch 1 has the reference particle position of -0.28 mm and peak current of 804 A, and bunch 2 has reference particle position of -0.06 mm and peak current of 1115 A. Delay between the two bunches is around 220 µm and both bunches present similar shaping as shown in Fig. 1. The overcompression is shown by the longitudinal phase space. The slice emittance is around 0.6 mm mrad. .

Table 1: Start-to-end Simulation Parameters

Parameter	Bunch 1	Bunch 2	Unit
Electron beam			
Charge	250	250	pC
s_0	8.5	0	mm
ζ_0	0.0064	0.0002	
ζ_1	-0.658	4.284	m^{-1}
ζ_2	-1074	-1058	m^{-2}
ζ_3	1.8×10^6	1.6×10^6	m^{-3}
C^0_{BC1}	1.89	4.48	
C^0_{BC2}	-27	-45	
C'^0_{BC2}	-3.1×10^5	6.5×10^5	m^{-1}
C''^0_{BC2}	-2.6×10^9	-2.0×10^{10}	m^{-2}
Bunch compressor			
$R_{56,LH+BC1}$	-217		mm
$T_{566,LH+BC1}$	360		mm
$R_{56,BC2}$	-94		mm
$T_{566,BC2}$	143		mm
rf			
V_{11}	147.6		MV
ϕ_{11}	-1.23		deg
V_{13}	20.9		MV
ϕ_{13}	159.7		deg
V_2	438.3		MV
ϕ_2	21.5		deg

CONCLUSION AND OUTLOOK

In conclusion, twin-bunch modelling in linear accelerators is studied and start-to-end simulations for the FLASH accelerator are carried out. It is shown that beam shaping may be achieved by utilizing a temporally shaped initial twin-bunch distribution, along with precise control over the acceleration and compression processes in the linac. Twin-bunch generation directly from the photocathode automatically applies to high-repetition rate operation mode. A well-controlled twin-bunch acceleration can benefit PWFA, hence further FEL and high-energy physics applications in the existing linacs. The collective effects will be included in the modelling in future studies, which can provide a better control over twin-bunch shaping and delay. The precise control is essential especially for high current operation modes, such as for the European XFEL case [21].

ACKNOWLEDGEMENTS

We would like to thank I. Zagorodnov for providing the original start-to-end simulation scripts. We acknowledge helpful discussions with S. Tomin, M. Dohlus and D. Samoilenko.

ISBN: 978-3-95450-248-6 ISSN: 2673-5490 doi: 10.18429/JACoW-IPAC25-TUPM089

REFERENCES

[1] A. Marinelli *et al.*, "High-intensity double-pulse X-ray free-electron laser,"*Nat. Commun.*, vol. 6, no. 1, Mar. 2015. doi:10.1038/ncomms7369

[2] Z. Zhang, Y. Ding, A. Marinelli, and Z. Huang, "Longitudinal dynamics of twin electron bunches in the Linac Coherent Light Source", *Phys. Rev. Spec. Top. Accel Beams*, vol. 18, no. 3, Mar. 2015. doi:10.1103/physrevstab.18.030702

[3] C. Emma *et al.*, "Free electron lasers driven by plasma accelerators: status and near-term prospects", *High Power Laser Sci. Eng.*, vol. 9, 2021. doi:10.1017/hpl.2021.39

[4] R. Pompili *et al.*, "Free-electron lasing with compact beam-driven plasma wakefield accelerator,"*Ann. Sci. Nat. Zool. Biol. Anim.*, vol. 605, no. 7911, pp. 659–662, May 2022. doi:10.1038/s41586-022-04589-1

[5] C. A. Lindström *et al.*, "Beam-driven plasma-wakefield acceleration", *arXiv:2504.05558, 2025*. doi:10.48550/arXiv.2504.05558

[6] R. D'Arcy*et al.*, "Recovery time of a plasma-wakefield accelerator", *Ann. Sci. Nat. Zool. Biol. Anim.*, vol. 603, no. 7899, pp. 58–62, Mar. 2022. doi:10.1038/s41586-021-04348-8

[7] J. Wood *et al.*, "Progress towards high-quality, high-repetition-rate plasma acceleration at FLASHForward", in *Proc. IPAC'24*, Nashville, TN, USA, May 2024, pp. 541–544. doi:10.18429/JACoW-IPAC2024-MOPR40

[8] D. Bazyl, Y. Chen, M. Dohlus, and T. Limberg, "CW operation of the European XFEL: SC-gun injector optimization, S2E calculations, and SASE performance", *arXiv:2111.01756, 2021*. doi:10.48550/arXiv.2111.01756

[9] S. Schröder *et al.*, "Tunable and precise two-bunch generation at FLASHForward", *J. Phys. Conf. Ser.*, vol. 1596, no. 1, p. 012002, Jul. 2020. doi:10.1088/1742-6596/1596/1/012002

[10] M. Tzoufras *et al.*, "Beam Loading in the Nonlinear Regime of Plasma-Based Acceleration", *Phys. Rev. Lett.*, vol. 101, no. 14, Sep. 2008. doi:10.1103/physrevlett.101.145002

[11] G. Loisch *et al.*, "Observation of High Transformer Ratio Plasma Wakefield Acceleration", *Phys. Rev. Lett.*, vol. 121, no. 6, Aug. 2018. doi:10.1103/physrevlett.121.064801

[12] W. H. Tan, P. Piot, and A. Zholents, "Formation of temporally shaped electron bunches for beam-driven collinear wakefield accelerators", *Phys. Rev. Accel. Beams*, vol. 24, no. 5, May 2021. doi:10.1103/physrevaccelbeams.24.051303

[13] C. A. Lindstrøm *et al.*, "Energy-Spread Preservation and High Efficiency in a Plasma-Wakefield Accelerator", *Phys. Rev. Lett.*, vol. 126, no. 1, Jan. 2021. doi:10.1103/physrevlett.126.014801

[14] W. Ackermann *et al.*, "Operation of a free-electron laser from the extreme ultraviolet to the water window", *Nat. Photonics*, vol. 1, no. 6, pp. 336–342, Jun. 2007. doi:10.1038/nphoton.2007.76

[15] "FLASH2020+ Conceptual Design Report (CDR)", DESY, Germany, Jan. 2020. doi:10.3204/PUBDB-2020-00465

[16] I. Zagorodnov and M. Dohlus, "Semianalytical modeling of multistage bunch compression with collective effects", *Phys. Rev. Spec. Top. Accel Beams*, vol. 14, no. 1, Jan. 2011. doi:10.1103/physrevstab.14.014403

[17] I. Zagorodnov, M. Dohlus, and S. Tomin, "Accelerator beam dynamics at the European X-ray Free Electron Laser,"*Phys. Rev. Accel. Beams*, vol. 22, no. 2, p. 024401, Feb. 2019. doi:10.1103/physrevaccelbeams.22.024401

[18] E. Schneidmiller and I. Zagorodnov, "Two-bunch seeding of soft x-ray free electron lasers", *Phys. Rev. Accel. Beams*, vol. 27, no. 11, Nov. 2024. doi:10.1103/physrevaccelbeams.27.110703

[19] K. Floettmann*et al.*, "ASTRA: A space charge tracking algorithm", DESY, Germany, 2017.

[20] I. Agapov, G. Geloni, S. Tomin, and I. Zagorodnov, "Ocelot: A software framework for synchrotron light source and fel studies", *Nucl. Instrum. Methods Phys. Res. A*, vol. 768, pp. 151–156, 2014. doi:10.1016/j.nima.2014.09.057

[21] W. Decking *et al.*, "A MHz-repetition-rate hard X-ray free-electron laser driven by a superconducting linear accelerator", *Nat. Photonics*, vol. 14, no. 6, pp. 391–397, 2020. doi:10.1038/s41566-020-0607-z